AlGaN/GaN HEMTs—An Overview of Device Operation and Applications

UMESH K. MISHRA, FELLOW, IEEE, PRIMIT PARIKH, AND YI-FENG WU

Invited Paper

Wide bandgap semiconductors are extremely attractive for the gamut of power electronics applications from power conditioning to microwave transmitters for communications and radar. Of the various materials and device technologies, the AlGaN/GaN high-electron mobility transistor seems the most promising. This paper attempts to present the status of the technology and the market with a view of highlighting both the progress and the remaining problems.

Keywords*—*Gallium nitride, high-electron mobility transistor (HEMTs), MMICs, polarization.

I. Introduction and Market Analysis

As the market for cellular, personal communications services, and broad-band access are expanding and third-generation (3G) mobile systems coming closer to reality, radio frequency (RF) and microwave power amplifiers are beginning to be the focus of attention. A variety of power-amplifier technologies are vying for market share, such as Si lateral-diffused metal–oxide–semiconductors and bipolar transistors, GaAs metal–semiconductor field-effect transistors (MESFETs), GaAs (or GaAs/InGaP) heterojunction bipolar transistors, SiC MESFETs, and GaN high-electron mobility transistors (HEMTs).

The materials properties of GaN compared to the competing materials is presented in Table 1. The resulting competitive advantages of GaN devices and amplifiers for a commercial product are described in Table 2. The first column states the required performance benchmarks for any technology for power devices and the second column lists the enabling feature of GaN-based devices that fulfill this need. In every single category, GaN devices excel over conventional technology. The last column summarizes the resulting performance advantages at the system level and to the customer. The highlighted features offer the most significant product benefits. The high power per unit width translates into smaller devices that are not only easier to fabricate, but also offer much higher impedance. This makes it much easier to match them to the system, which is often a complex task with conventional devices in GaAs (for e.g., a matching ratio ten times larger might be needed for a GaAs transistor, increasing overall complexity and cost). The high-voltage feature eliminates or at least reduces the need for voltage conversion. Commercial systems (e.g., wireless base station) operate at 28 V and a low-voltage technology would need voltage step down from 28 V to the required voltage. However, GaN devices can easily operate at 28 V and potentially up to 42 V. The higher efficiency that results from this high operating voltage reduces power requirements and simplifies cooling, an important advantage, since cost and weight of cooling systems is a significant fraction of the cost of a high-power microwave transmitter. The nitride technology is also the critical enabler for blue, green, and white lighting. The commercial lighting market is a multibillion dollar market. While some of the requirements for RF and microwave applications are different (such as the need for a semiinsulating substrate), there is no doubt that exercising

Table 1
Table of Properties of Competing Materials in Power Electronics

Material	μ	ε	Eg	BFOM Ratio	JEM Ratio	Tmax
Si	1300	11.4	1.1	1.0	1.0	300 C
GaAs	5000	13.1	1.4	9.6	3.5	300 C
SiC	260	9.7	2.9	3.1	60	600 C
GaN	1500	9.5	3.4	24.6	80	700 C

Manuscript received October 4, 2001; revised January 26, 2002. This work was supported by the Office of Naval Research, Air Force Office of Scientific Research, Defense Advanced Research Projects Agency, Ballistic Missile Defense Organization, and Small Business Innovative Research programs.

U. K. Mishra is with the Electrical and Computer Engineering Department, Engineering I, University of California, Santa Barbara, Santa Barbara, CA 93106 USA.

P. Parikh and Y.-F. Wu are with Cree Lighting Company, Goleta, CA 93117 USA.

Publisher Item Identifier S 0018-9219(02)05582-2.

Table 2
Competitive Advantages of GaN Devices

Need	Enabling Feature	Performance Advantage
High Power/Unit Width	Wide Bandgap, High Field	Compact, Ease of Matching
High Voltage Operation	High Breakdown Field	Eliminate/Reduce Step Down
High Linearity	HEMT Topology	Optimum Band Allocation
High Frequency	High Electron Velocity	Bandwidth, μ-Wave/mm-Wave
High Efficiency	High Operating Voltage	Power Saving, Reduced Cooling
Low Noise	High Gain, High Velocity	High dynamic range receivers
High Temperature Operation	Wide Bandgap	Rugged, Reliable, Reduced Cooling
Thermal Management	SiC Substrate	High Power Devices with Reduced Cooling Needs
Technology Leverage	Direct Bandgap Enabler for Lighting	Driving Force for Technology: Low Cost

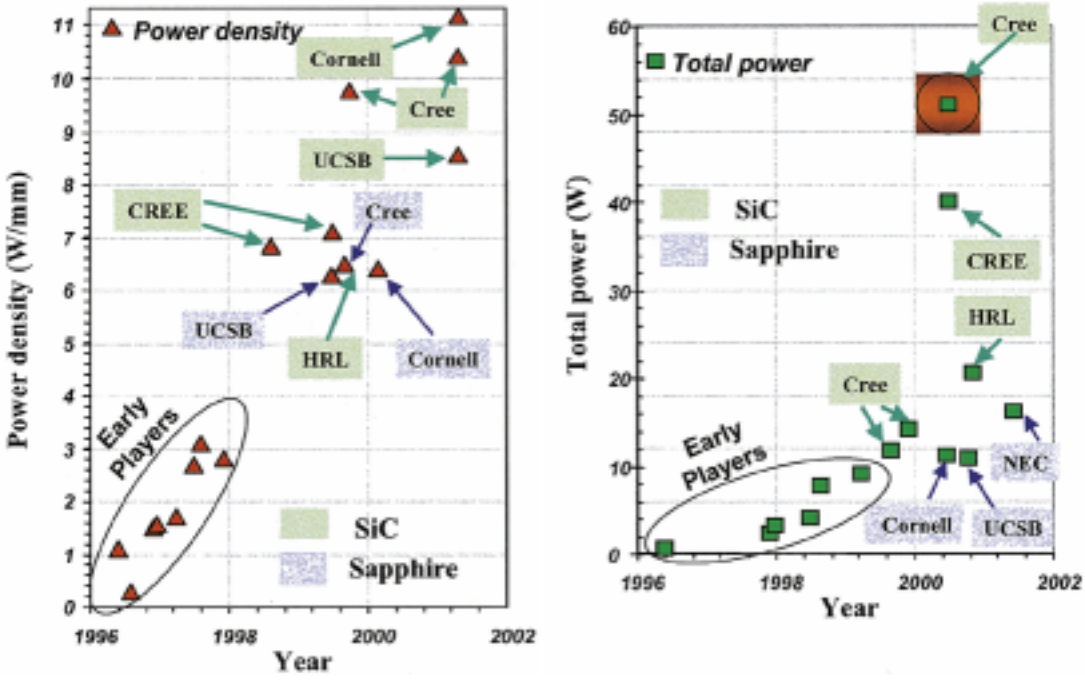

(a) (b)

Fig. 1. Historical progress in GaN transistor technology. (a) Power density of AlGaN/GaN HEMTs versus year. (b) Total power of AlGaN/GaN HEMTs versus year.

overlapping technologies will contribute in driving the development cost down of RF components and offer leverage up to a certain extent.

The rate of progress in the power density and total power available from AlGaN/GaN HEMTs has been remarkable, as shown in Fig. 1. This has increased confidence in considering GaN HEMTs for commercial and Department of Defense applications, sooner rather than later. GaN HEMTs have demonstrated one-order higher power density and higher efficiency over the existing technologies—Si- and GaAs-based RF and microwave transistors. Thus, for the same output power, a ten times reduction in device size can be realized using GaN-based devices in place of conventional devices. The schematic of Fig. 2 illustrates this case, where a complex module can potentially be replaced by a smaller module utilizing GaN. In this case, having higher power per unit die of GaN would not only translate to lower chip costs, but also contribute to reduced system costs by reducing/eliminating power combining.

The above technological advantages result from the combination of the wide bandgap of GaN and the availability of the AlGaN/GaN heterostructure where high voltage, high current, and low on-resistance can be simultaneously achieved, resulting in high-power high-efficiency operation.

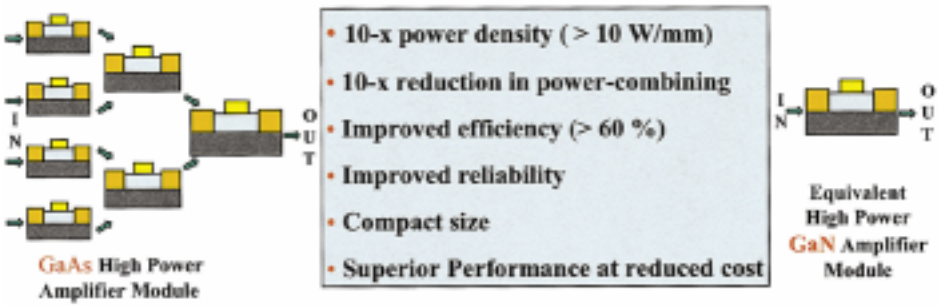

Fig. 2. Schematic comparison illustrating advantages of GaN over existing technology.

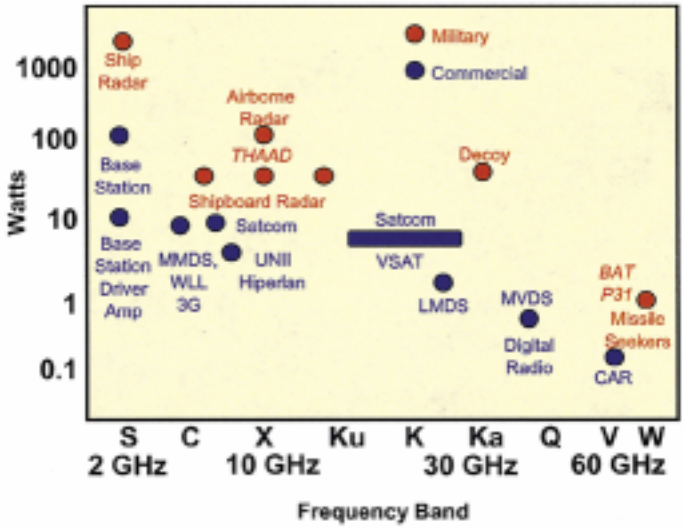

Fig. 3. Applications for GaN HEMTs.

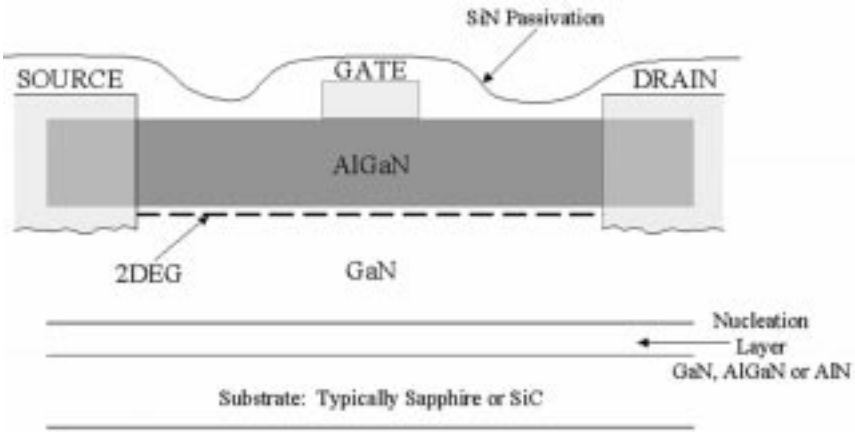

Fig. 4. Basic HEMT structure.

Furthermore, the wide bandgap offers a rugged and reliable technology capable of high-voltage high-temperature operation. This opens up several industrial, automotive, and aircraft applications, such as power and high-voltage rectifiers and converters. Some of the commercial and military markets that can be targeted by GaN are shown in Fig. 3.

According to a recent survey by Strategies Unlimited, the total GaN electronic-device market is expected to reach U.S. $500 million by the end of this decade. RF and microwave applications are likely to be the largest share of the GaN device market. The GaN HEMT targets both military and commercial applications. The former includes radar (shipboard, airborne, and ground) and high-performance space electronics. The latter includes base-station transmitters, C band Satcom, Ku–K band very small apperture terminal and broad-band satellites, local multipoint distribution systems, and digital radio.

II. Device Structure and Materials Issues

Fig. 4 shows the structure of a basic HEMT. The lack of a GaN substrate necessitates heteroepitaxy on compatible

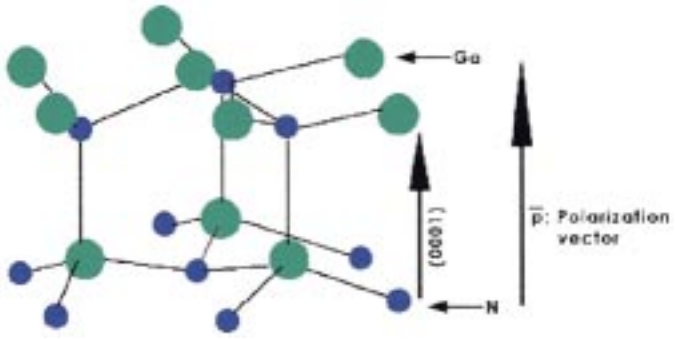

Fig. 5. Crystal structure of Ga-polarity or Ga-face GaN.

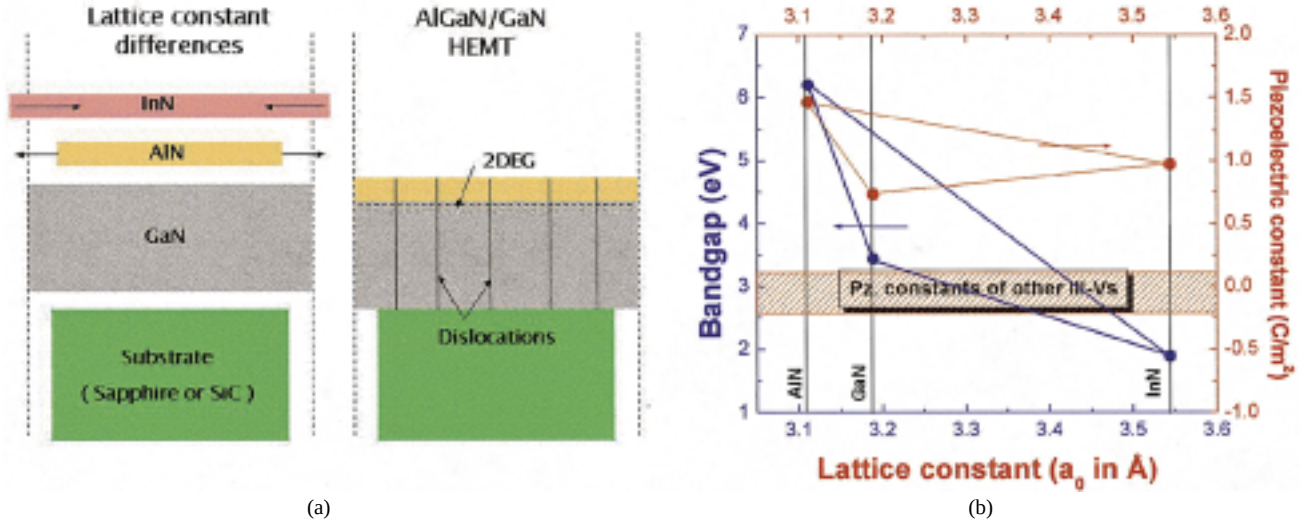

(a) (b)

Fig. 6. (a) Band diagram and (b) piezoelectric polarization versus the lattice constant for (Al, Ga, In, N) system.

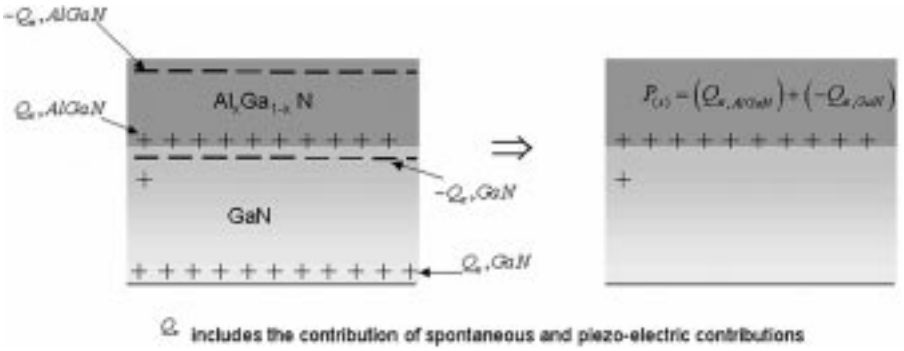

(a)

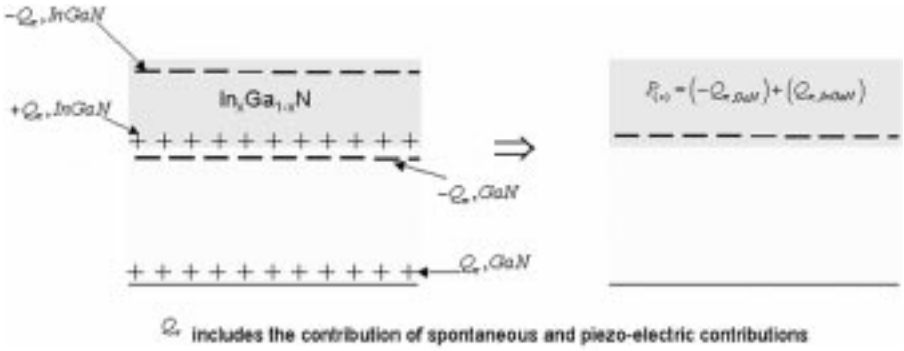

(b)

Fig. 7. (a) Net positive charge at the AlGaN/GaN interface caused by the sum of the net spontaneous polarization and piezoelectric polarization between AlGaN and GaN. (b) Net negative charge at the In GaN–GaN interface caused by the compressive strain resulting from growth of $In_xGa_{1-x}N$ on GaN.

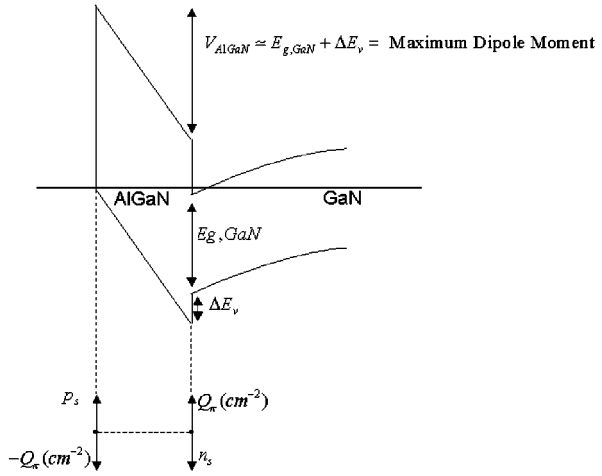

(a)

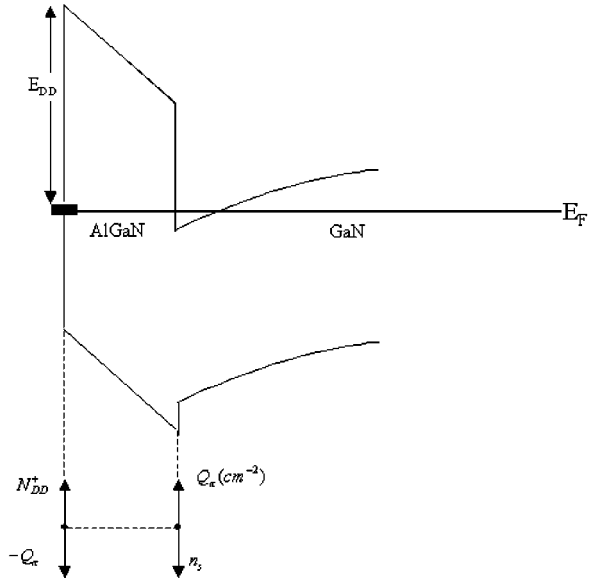

(b)

Fig. 8. (a) Band diagram of the AlGaN–GaN HEMT if the polarization dipole is partially terminated by a surface hole gas. (b) Band diagram of the AlGaN–GaN HEMT if the polarization dipole is partially terminated by a surface deep donor.

substrates, commonly sapphire and SiC, but AlN, Si, and complex oxides such as LiG may also emerge as viable. The epitaxial layers may be either grown entirely by molecular beam epitaxy or metal-organic chemical vapor deposition (MOCVD) or on a resistive GaN buffer grown by vapor phase epitaxy, though the latter, currently, is less common. Heteroepitaxy on such severely lattice-mismatched substrates makes the nucleation layer one of the most critical aspects of the growth. With sapphire as a substrate, the nucleation layer consists of GaN or AlN deposited at a low temperature (typically 600 °C), which is then heated up to the growth temperature of the main layer [1]. The GaN and AlGaN layers are typically grown at 1000 °C at growth rates of $\sim$1 μm/h. Nucleation on SiC is typically performed using AlN grown at 900 °C [2].

A physical effect that dominates device behavior and may also determine defect density in the film is the polar nature

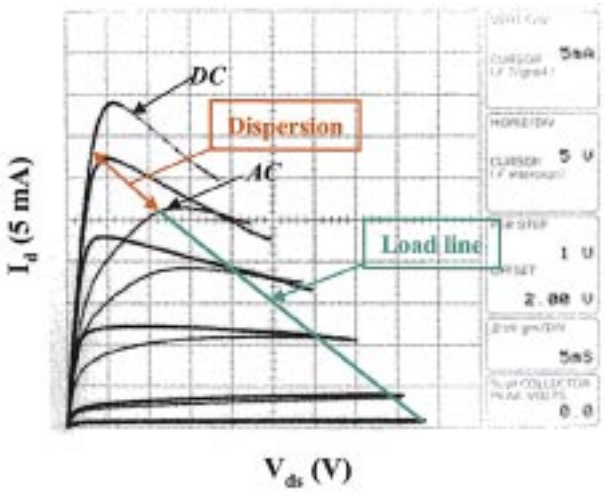

Fig. 9. Dispersion between the large-signal ac and dc HEMT characteristics simulated by a 80 μs pulse on the gate.

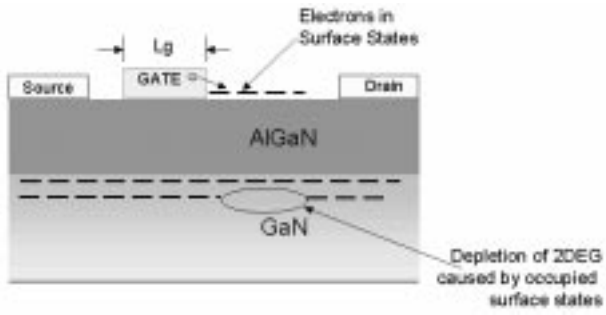

Fig. 10. Proposed mechanism for large-signal dispersion. Occupancy of surface traps under negative bias.

of the GaN and AlGaN. Fig. 5 shows the crystal structure of Ga-polarity or Ga-face GaN. Currently, all high-quality material is grown with this polarity. The sense of the spontaneous polarization is indicated on the diagram. The band diagram and piezoelectric constants versus lattice constant for the (Al, Ga, In, N) system is shown in Fig. 6. The tensile strain caused by the growth of $Al_xGa_{1-x}N$ on GaN results in a piezoelectric polarization P_{pz} that adds to the net spontaneous polarization P_{sp} in a manner given by [3]

$$\begin{aligned} P(x) &= P_{pz} + P_{sp} \\ &= -[(3 \cdot 2x - 1 \cdot 9x^2) \\ &\quad \times 10^{-6} - 5 \cdot 2 \times 10^{-6}x]C\ \mathrm{cm}^{-2} \end{aligned}$$

where $P_{(x)}$ is the net total polarization. This results in a net positive charge at the AlGaN/GaN interface, as shown in Fig. 7(a). The compressive strain caused by the growth of $In_xGa_{1-x}N$ on GaN causes a net negative piezoelectric polarization charge at the $In_xGa_{1-x}N$–GaN interface, as shown in Fig. 7(b). The magnitude of the charge follows [3]

$$\begin{aligned} P(x) &= P_{pz} + P_{sp} \\ &= [(14 \cdot 1x + 4 \cdot 9x^2) \\ &\quad \times 10^{-6} - (0 \cdot 3 \times 10^{-6})x]C\ \mathrm{cm}^{-2}. \end{aligned}$$

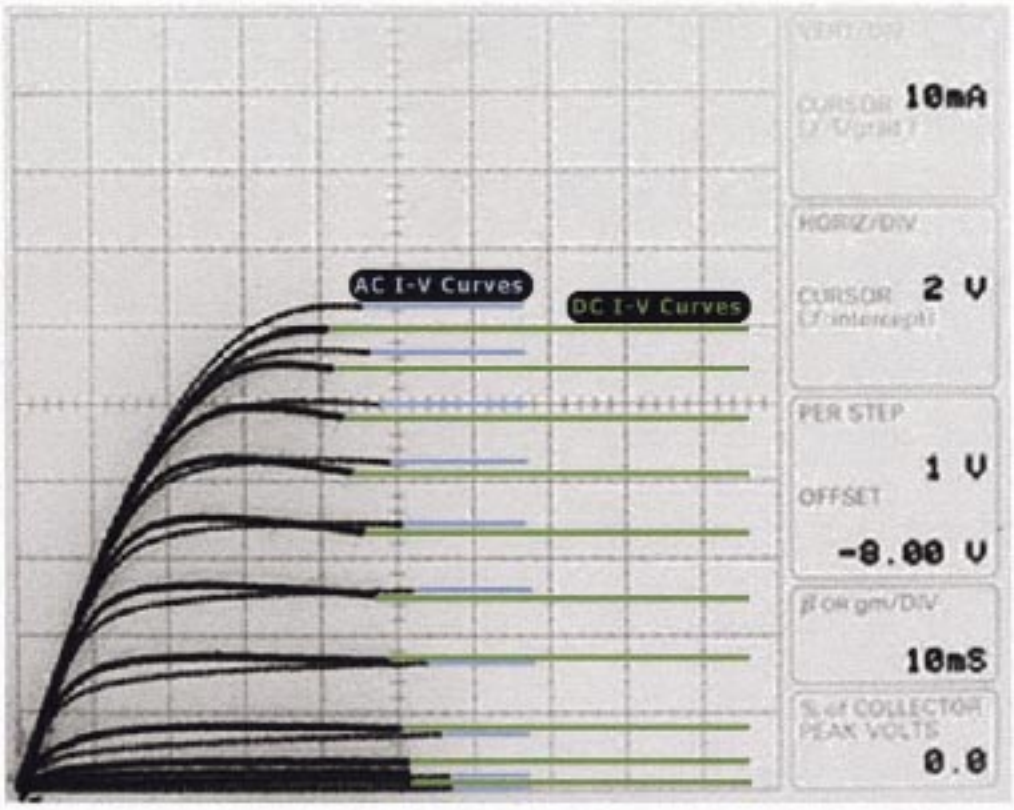

Fig. 11. SiN passivation eliminating reduced channel current and higher on-resistance (symptoms of dispersion).

The built-in polarization dipole can have a maximum moment approximately equal to $\Delta E_v + E_{g,\,\mathrm{GaN}}$, as apparent from the band diagram in Fig. 8(a). The charge distribution is then composed of the polarization dipole $\pm Q_\pi$ and an opposing dipole comprising of a surface hole gas p_s and a two-dimensional electron gas (2DEG) at the heterointerface n_s. In practice, experiments [4] have shown that the 2DEG is induced before a surface hole gas formation by the ionization of a deep surface donor resulting in a charge distribution, shown in Fig. 8(b). Here, the polarization dipole is screened by the positively charged surface donor (of depth E_{DD} and concentrationN_{DD}^{+}) and the 2DEG.

III. Device Fabrication and Performance

Device fabrication of the AlGaN/GaN HEMT (shown in Fig. 4) commences with the definition of the active device area. This can be either determined by Cl_2 mesa-etching [5] or by the ion implantation [6]. Next, the ohmic contacts are formed by first, partially etching the AlGaN in the source and drain regions, depositing the ohmic metals and annealing at 900 °C. Though Ti/Al/Ni/Au has been the preferred metallurgy [7], Ta-based ohmic contacts [8] are now being investigated for their improved morphology. Next, the gate is defined by liftoff of Ni/Au metallurgy. The efficacy of a gate recess, which is commonly employed in compound semiconductor technology, is currently being investigated in the GaN system [9]. Device fabrication is completed with a deposition of a SiN passivation layer. This layer serves a critical purpose in eliminating dispersion between the large-signal alternating current (ac) and the direct current (dc) characteristics of the HEMT. The effect is illustrated in Fig. 9, where the ac curve is obtained by biasing the device into pinchoff and trying to recover the full channel current by pulsing the gate on by utilizing a 80-μs gate pulse on a curve tracer. The maximum ac is less than the dc, the difference being referred to as dispersion. This effect can be explained (though alternate plausible explanations are currently being discussed [10]) by the mechanism depicted in Fig. 10. When the device is biased into pinchoff, electrons from the gate are injected into the empty surface donors required to maintain a 2DEG. Compensation of these donors reduces the 2DEG. Under ac drive, the electrons cannot respond because of the long-time constant of the donor traps, resulting in a reduced channel current and higher on-resistance (symptoms of dispersion). SiN passivation eliminates this effect, as shown in Fig. 11, though the exact mechanism is under debate.

IV. Device and Circuit Performance

Typically, AlGaN/GaN HEMTs have demonstrated high-power densities of 6–9 W/mm both on sapphire and SiC substrates [11]–[13], approaching a one-order improvement over conventional HEMTs and confirming the extremely great potential of this device technology predicted by theory. However, these power density values were generally achieved under high gain compression of 5–9 dB, which is an indication of undesired nonlinearity. This phenomenon can be explained

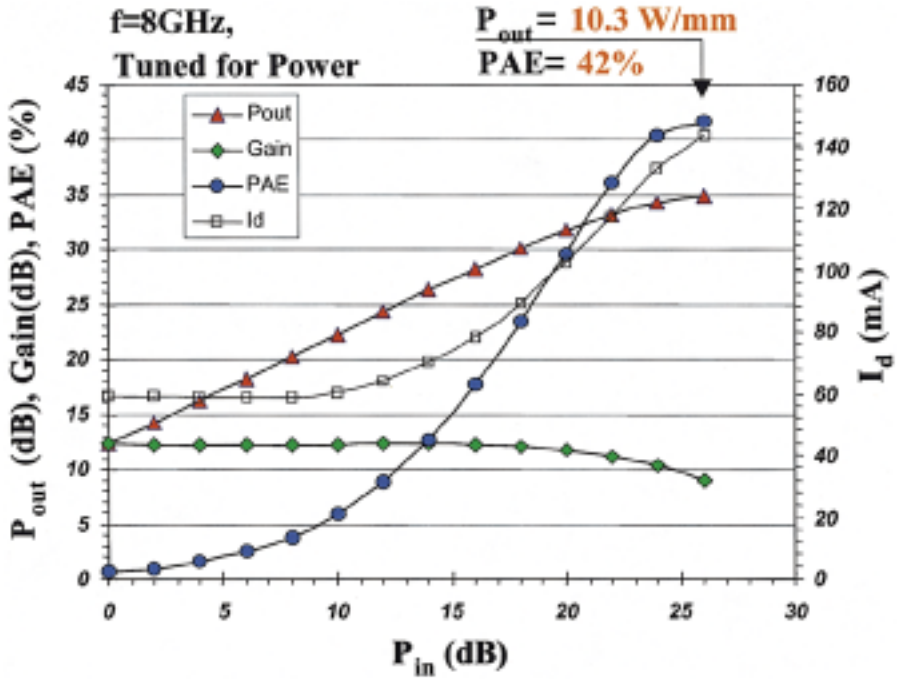

Fig. 12. Power performance of a 300-μm-wide AlGaN/GaN HEMT, showing 10.3-W/mm power density, the highest for any FET of the same size. Gain compression was -3.4 dB; drain bias was 45 V. Device dimension: 300×0.6 mm^2.

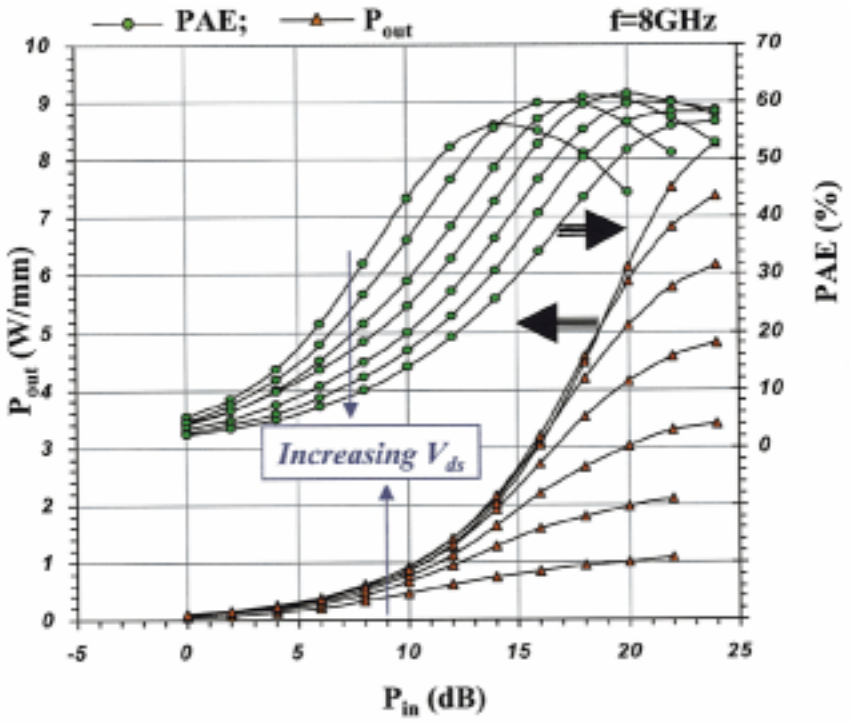

Fig. 13. Family of power sweeps at 8 GHz with biases of 10, 15, 20, 25, 30, 35, 40 V. A relatively flat PAE plateau of 56%–62% was achieved through out the wide voltage span. Device dimension: 300×0.6 mm^2. Tuning was performed at 35 V for optimum PAE.

by traps, although largely reduced, still existing in these devices. Recently, effort in pursuing higher quality epilayers of the AlGaN/GaN HEMTs has resulted in significant improvement of the large-signal characteristics. These devices were grown by MOCVD on semiinsulating SiC substrates. The epilayers consisted of an insulating GaN buffer and a lightly doped AlGaN layer to supply charge for the two-dimensional gas as well as to serve as a Schottky-gate barrier. The Al composition was greater than 30%. Special attention was paid to ensure high crystal quality of all the epilayers. Typical mobility was improved to >1500 cm^2/V·s from previous values around 1200 cm^2/V·s simultaneously with a high 2DEG density of

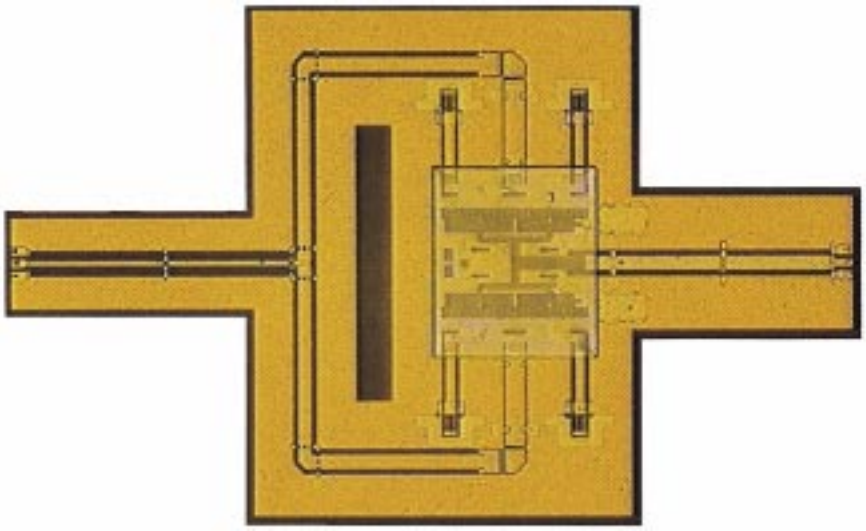

Fig. 14. Photo of a 50-W GaN-based flip-chip amplifier IC incorporating a 8-mm AlGaN/GaN HEMT. Circuit size is about 10 mm × 7 mm.

1–1.2 × 10^{13} cm^{-2}. The gatelength was 0.6 μm, obtained by optical stepper lithography. The gatewidth was 2 × 150 μm or 300 μm, with a U-shape layout.

The devices showed an on-resistance of 2.5 Ω-mm (after subtraction of the resistance due to the wire and probes) and a current density of 1 A/mm. The breakdown voltage was >80 V. The current-gain and power-gain cutoff frequencies were 25 and 60 GHz, respectively. An ATN Microwave load-pull system was used for large-signal characterization at 8 GHz. Fig. 12 shows the onwafer measurement result of a 300-μm-wide device when tuned for power. A power density of 10.3 W/mm was achieved along with 42% power-added efficiency (PAE). This increased power density was obtained at a reduced gain compression of 3.4 dB, which is attributed to reduction of trapping effect due to improved epi quality and surface passivation. Since the trapping effect deteriorates with increased electric field or bias voltage for a specific device dimension, performance of the devices as a function of bias voltage can be used as a valid measure of this phenomenon. Fig. 13 shows the measurement results of the AlGaN/GaN HEMTs under a wide voltage bias range from 10 to 40 V, where the tuning was for optimum efficiency. It is seen that a relatively flat PAE plateau of 56%–62% was achieved throughout the wide voltage span, illustrating flexibility of power-supply requirement for various applications. Simultaneously high-power density of 8.3 W/mm and PAE of 57% were obtained at 40-V bias. The ability to achieve a high PAE at such a high bias voltage confirms the reduction of trapping effect with these devices. Obtaining a high PAE simultaneously with high power is essential for system insertion since dealing with the heat generated in inefficient amplifiers could be prohibitively difficult.

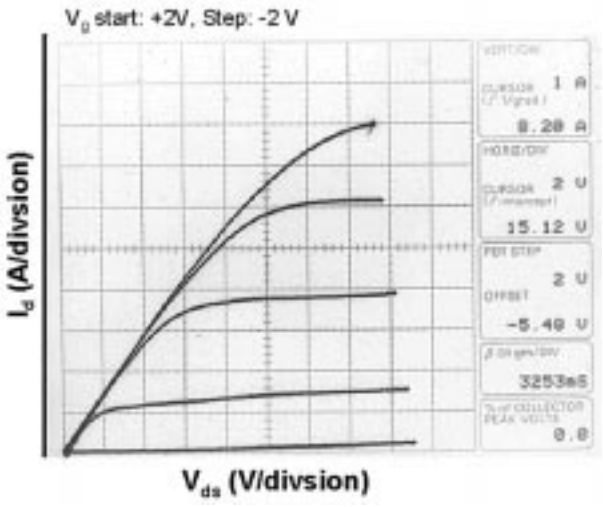

Fig. 15. I–V characteristics of the 8-mm AlGaN/GaN HEMT, showing a maximum current level of 8 A. Most of the apparent on-resistance was due to the resistance of wire and probes.

V. GaN-Based Amplifiers

The design of a GaN-based power amplifier is significantly different from the conventional GaAs-based one in a sense that both the input and output impedance transformation ratios are drastically reduced for the same output power rating. With a gate length of 0.6 μm, maximum drain current of 1 A/mm, and a breakdown voltage of 80 V, an AlGaN/GaN HEMT typically shows an input capacitance of 2.7 pF/mm, similar to that of a GaAs-based HEMT, while the optimum output load is 75 Ωmm, about two times that of a GaAs HEMT. Since the GaN HEMT offers ten times the power density for the same output power, the input transformation ratio is ten times less, while the output is twenty times less than a GaAs HEMT. For high-power amplifiers where multimillimeter to centimeter gate peripheries are needed, this reduction in impedance transformation translates to great circuit matching simplicity. Another design difference lies in the high operation voltage of these devices, which requires higher voltage ratings of the onchip capacitors.

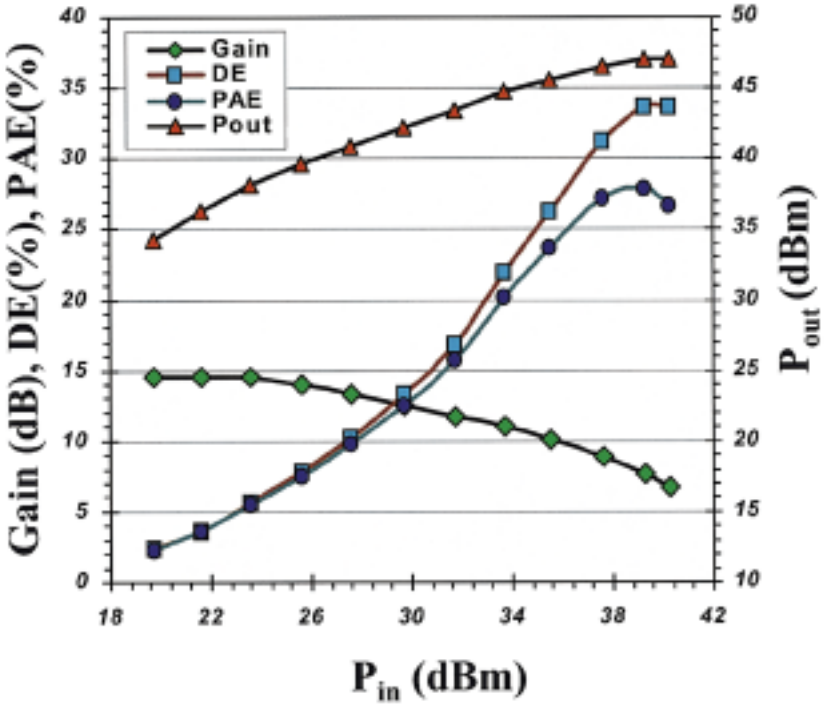

Fig. 16. Power sweep of the GaN FC-IC at 6 GHz, showing a peak output of 47.1 dB or 51 W, the highest achieved for an 8-mm solid-state FET to date.

A C-band power amplifier is illustrated below to show the benefit of using the AlGaN/GaN HEMT. Taking into account device nonuniformity, drive nonuniformity and circuit loss, a total gate periphery of 8 mm was chosen to achieve a design goal of 50-W output. At the input, a capacitance–inductance–equilibrium–resistance network was used to convert the capacitive gate impedance to a real value of about 1.5 Ω within the bandwidth. This was then transformed to the 50-Ω input impedance by a multiple π network. At the output, the power load for the 8-mm-wide device was about 7.5 W (assuming a bias of 35 V and a knee voltage of 5 V), which was transformed to the 50-W circuit output. The circuit was laid out in a coplanar-wave transmission line system and constructed using a flip-chip integrated-circuit scheme (FC-IC). The circuit substrate was AlN, on which all metal–insulator–metal capacitors, metal resistors, and air-bridge interconnects were fabricated as integrated components. The devices were diced and flip-chip-bonded onto the circuit substrates for optimum electrical and thermal interfacing. The finished FC-IC amplifier is shown in Fig. 14. The output characteristics of the device are shown in Fig. 15. The maximum current of 8 A indicates satisfactory electrical scaling, which is crucial for achieving desired output power. The amplifier exhibited a midband small-signal gain 14.5 dB when biased above 25 V, close to the simulation result of 16 dB. Pulsed-power measurement was performed using 0.5-mS pulsewidth and 5% duty cycle. The output power at 6 GHz was 35 W when biased at 29 V, which increased to 49 W at 38 V. At 39 V, an output power of 51 W at 6 GHz was recorded as shown in Fig. 16. This represents a remarkable power level for a solid-state FET with a gatewidth of only 8 mm. The corresponding power density was 6.4 W/mm. For the same output value in the conventional GaAs-based FET technology, either a HEMT or a MESFET, the device gate periphery would have been 80 mm and require a challenging input impedance transformation from 0.15 to 50 Ω!

VI. Summary and Conclusion

While GaN device and circuit technology is likely poised to break out in the commercial arena, certain risks or barriers to entry in the market should not be overlooked. The relative technology immaturity of GaN with respect to Silicon and GaAs leave issues like long-term reliability unanswered. The market pull in the acceptance of a new technology might be weak. For example, it might be difficult to get into the design cycles of some of the products like 3G base-station amplifiers early enough to be the technology of choice when these systems are eventually deployed. Finally, the relative high initial cost will continue to be an issue. Most of the promising results for GaN have been achieved on semiinsulating SiC substrates, which are currently commercially available only at 2-in diameter. However, wafer vendors are aggressively working on higher diameter wafers.

With all of these in mind, the overall performance advantages for early insertion of GaN will have to be compelling to justify the higher cost product. Initially, GaN will be a replacement technology and vie to take markets from existing technologies including existing solid-state Si- and GaAs-based solutions, as well as high-power microwave vacuum tubes. Ultimately, the compact size of GaN-based

transistors will lead to lower cost products. This will increase system efficiency, reduce system costs, and expand the market applications.

ACKNOWLEDGMENT

The authors would like to thank Dr. S. Keller, Prof. S. DenBaars, and Prof. J. Speck and the authors' students and colleagues who made the progress possible.

REFERENCES

[1] H. Amano, N. Sawaki, I. Akasaki, and Y. Toyoda, "Metalorganic vapor phase epitaxial growth of high quality GaN film using an AlN buffer layer," *Appl. Phys. Lett.*, vol. 48, no. 5, pp. 353–355, Feb. 1986.

[2] T. W. Weeks, Jr., M. D. Bremser, K. S. Ailey, E. Carlson, W. G. Perry, and R. F. Davis, "GaN thin films deposited via organometallic vapor phase epitaxy on alpha (6H)-SiC(0001) using high-temperature monocrystalline AlN buffer layers," *Appl. Phys. Lett.*, vol. 67, pp. 401–403, July 1995.

[3] O. Ambacher, J. Smart, J. R. Shealy, N. G. Weimann, K. Chu, M. Murphy, W. J. Schaff, L. F. Eastman, R. Dimitrov, L. Wittmer, M. Stutzman, W. Rieger, and J. Hilsenbeck, "Two-dimensional electron gases induced by sontaneous and piezoelectric polarization charges in N- and Ga-face AlGaN/GaN heterostructures," *J. Appl. Phys.*, vol. 85, no. 6, pp. 3222–3333, Mar. 1999.

[4] R. Vetury, N.-Q. Zhang, S. Keller, and U. K. Mishra, "The impact of surface states on the DC and RF characteristics of AlGaN/GaN HFETs," *IEEE Trans. Electron Devices*, vol. 48, pp. 560–566, Mar. 2001.

[5] S. J. Pearton, J. C. Zolper, R. J. Shul, and F. Ren, "GaN: Processing, defects, and devices," *J. Appl. Phys.*, vol. 86, no. 1, pp. 1–78, July 1999.

[6] S. C. Binari, H. B. Dietrich, G. Kelner, L. B. Rowland, K. Doverspike, and D. K. Wickenden, "H, He, and N implant isolation of n-type GaN," *J. Appl. Phys.*, vol. 78, no. 5, pp. 3008–3011, Sept. 1995.

[7] Z. Fan, S. N. Mohammand, W. Kim, O. Aktas, A. E. Botchkarev, and H. Morkoc, "Very low resistance ohmic contact to n-GaN," *Appl. Phys. Lett.*, vol. 68, no. 12, pp. 1672–1674, Mar. 1996.

[8] D. Qiao, L. Jia, L. S. Yu, P. M. Asbeck, S. S. Lau, S.-H Lim, Z. Liliental-Weber, T. E. Haynes, and J. B. Barner, "Ta-based interface ohmic contacts to AlGaN/GaN heterostructures," *J. Appl. Phys.*, vol. 89, no. 10, pp. 5543–5546, May 2001.

[9] D. Buttari, A. Chini, G. Meneghesso, E. Zanoni, P. Chavarkar, R. Coffie, N. Q. Zhang, S. Heikman, L. Shen, H. Xing, C. Zheng, and U. K. Mishra, "Systematic characterization of Cl_2 reactive ion etching for gate recessing in AlGaN/GaN HEMTs," *IEEE Electron Device Lett.*, vol. 23, pp. 118–120, Mar. 2002.

[10] G. Simm, A. Koudymox, A. Tarakji, X. Hu, J. Yang, M. A. Khan, M. S. Shur, and R. Gaska, "Induced strain mechanism of current collapse in AlGaN/GaN heterostructure field-effect transistor," *Appl. Phys. Lett.*, vol. 79, pp. 2651–2653, Oct. 2001.

[11] S. Keller, Y.-F. Wu, G. Parish, N. Zhang, J. J. Xu, B. P. Keller, S. P. DenBaars, and U. K. Mishra, "Gallium nitride based high power heterojunction field effect transistor: Process development and present status at UCSB," *IEEE Trans. Electron Devices*, vol. 48, pp. 552–559, Mar. 2001.

[12] S. T. Sheppard, K. Doverspike, W. L. Pribble, S. T. Allen, and J. W. Palmour, "High power microwave GaN/AlGaN HEMTs on silicon carbide," *IEEE Electron Device Lett.*, vol. 20, pp. 161–163, Apr. 1999.

[13] Y.-F. Wu, D. Kapolnek, J. P. Ibbetson, P. Parikh, B. P. Keller, and U. K. Mishra, "Very-high power density AlGaN/GaN HEMTs," *IEEE Trans. Electron Devices*, vol. 48, pp. 586–590, Mar. 2001.

Umesh K. Mishra (Fellow, IEEE) received the B.Tech. degree from the Indian Institute of Technology, Kanpur, India, in 1979, the M.S. degree from Lehigh University, Bethlehem, PA, in 1980, and the Ph.D. degree from Cornell University, Ithaca, NY, in 1984, all in electrical engineering.

He has been with various laboratory and academic institutions, including Hughes Research Laboratories, Malibu, CA, University of Michigan at Ann Arbor, and General Electric, Syracuse, NY, where he has made major contributions to the development of AlInAs–GaInAs high-electron mobility transistors and heterojunction bipolar transistors. He is currently a Professor with the Department of Electrical and Computer Engineering, University of California at Santa Barbara. He has authored or coauthored over 400 papers in technical journals and conferences and holds six patents. His current research interests include oxide-based III–V electronics and III–V nitride electronics and optoelectronics.

Dr. Mishra received the Young Scientist Award at the International Symposium on GaAs and Related Compounds and coreceived the Hughes Aircraft Patent Award.

Primit Parikh received the B.Tech. degree in electrical engineering from Indian Institute of Technology, Bombay, India, in 1993 and the M.S. and Ph.D. degrees in electrical and computer engineering from the University of California, Santa Barbara, in 1994 and 1998, respectively.

He has been with the Cree Lighting Company, Goleta, CA, since 1998, where he is currently a Manager of the GaN Electronics Program and has previously been involved with project management, reesource planning and forecasting, marketing, intellectual propoerty, and the core nitride technology. He has over eight years experience in semiconductor technology, including materials, devices, and circuits. His dissertation, which addressed high-efficiency power amplification, led to the fabrication of record high-efficiency GaAs-on-insulator transistors. He has authored or coauthored over 40 technical publications, conferences, and invited presentations, and two patents and and two patents pending.

Yi-Feng Wu received his B.E. degree in engineering thermal physics from Tsinghua University, Beijing, China, in 1985 and the M.S. degree in mechanical engineering and the Ph.D. degree in electrical engineering from the University of California, Santa Barbara, in 1994 and 1997, respectively.

His experiences ranged from traditional thermal engineering to submicrometer thermal imaging, from solid-state devices to microwave circuits. He is currently a Research Scientist on GaN-based device and amplifiers with the Cree Lighting Company, Goleta, CA. His dissertation was titled "Microwave Power AlGaN/GaN High-Mobility-Transistors." He has authored or coauthored more than 35 technical journal papers and conference presentations.